

NUMERICAL INVESTIGATION OF FLUID FLOW IN RADIAL DIFFUSERS WITH IRREGULAR BOUNDARIES

Viviana Cocco Mariani

Programa de Pós-Graduação em Engenharia Mecânica – PUCPR
Rua Imaculada Conceição, 1155, Prado Velho, CEP: 81611-970, Curitiba, PR, Brasil
e-mail: viviana.mariani@pucpr.br

Alvaro Toubes Prata

Departamento de Engenharia Mecânica, Universidade Federal de Santa Catarina – UFSC
CEP 88040-900, Florianópolis, SC, Brasil
e-mail: prata@mrva.ufsc.br

Abstract. Radial diffusers are the basic geometry for the automatic valves in reciprocating hermetic compressors. In the present work numerical solutions for the laminar isocoric flow in radial diffusers are performed to investigate the influence of some geometry modifications on the mass flow rate and on the resultant force on the valve. The numerical model was able to handle irregular geometries making use of a regular mesh, and was validated through comparisons with experiments. Results are presented in terms of the effective flow and force area of valves which are important efficiency parameters for the modelling and design of reciprocating hermetic compressors. The efficiency parameters are presented and explored in terms of small modification of the valve geometry, for Reynolds numbers varying from 1000 to 2500 and two values of the gap between valve reed and valve seat. The flow was significantly affected by the geometry modifications, indicating that with little effort the performance of automatic valves can be substantially improved. For instance, with a small chamfer of 5° at the outlet of the valve feeding orifice, the effective force area was increased by 30 percent.

Keywords: Radial diffuser, effective flow area, effective force area, hermetic compressor, ELAFINT

1. Introduction

The geometry of automatic valves in hermetic compressors can be approximated by a radial diffuser, as shown in Fig. 1. In this geometry the fluid flows axially through a feeding orifice with diameter d , and then is deflected along the radial direction by the frontal disk, represented in the figure by the valve reed with diameter D . In the present investigation the flow is assumed laminar and axially symmetric.

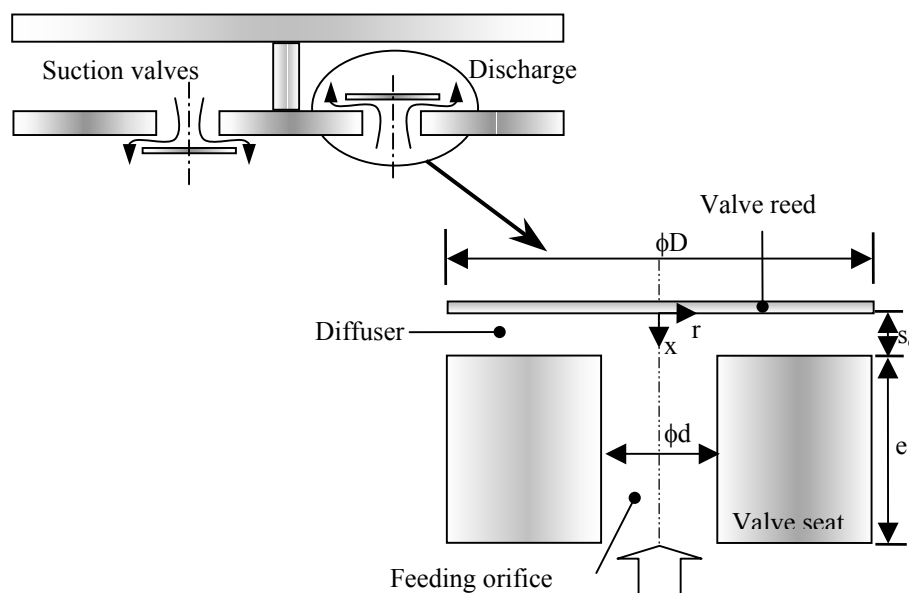


Figure 1. Concentric radial diffuser with parallel reed.

Both suction and discharge valves in hermetic compressors function according to the existing pressure difference between the interior of the cylinder and the suction and discharge chambers, respectively, and the opening and closing forces resulted from the pressure difference are dictated by the piston reciprocating movement. Geometrically, among

the main components that can be optimized in those valves are the dimensions and shape of the seat, feeding orifice and reed. Optimum valves operate at high efficiency which is evaluated by two parameters: effective flow and force areas. Those two parameters play an important role in modeling and designing of automatic valves.

Valve geometry has a significant influence on the effective flow and force areas, and one of the purposes of the present contribution is to investigate the influence of geometric parameters such as seat inclination and seat and reed radius on the effective flow and force areas. Figure 2 presents the four geometries for the radial diffuser investigated in the present work.

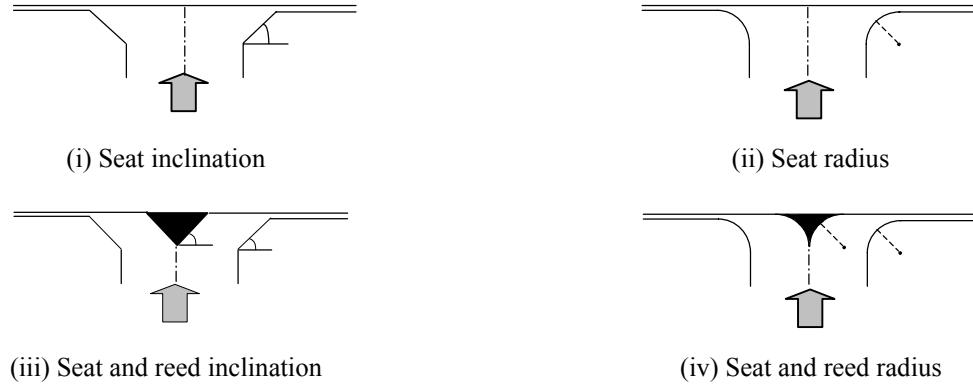


Figure 2. Geometry of radial diffuser with modified geometric parameters.

The literature on radial flow is extensive and some representative contributions are due to Hayashi *et al.* (1975), Ervin *et al.* (1989) and Tabatabai and Pollard (1987). For radial flow in the context of compressor valves the reader is referred to Ferreira and Driessen (1986), Ferreira *et al.* (1989), Prata and Ferreira (1990), Prata *et al.* (1995), Deschamps *et al.* (2000) and Possamai *et al.* (2001).

Ferreira and Driessen (1986) presented a discussion of the flow patterns encountered in reed type valves and reviewed the literature up to then. A numerical and experimental solution for the laminar isocoric flow field of air in radial diffusers, for small separation between discs, was explored by Prata *et al.* (1995), Ferreira *et al.* (1989) and Possamai *et al.* (2001). More recently numerical and experimental solutions for the turbulent flow has been presented by Deschamps *et al.* (2000). None of the previous work on radial diffuser investigated the geometric parameters explored in the present work.

The governing differential equations in cylindrical coordinates for the problem considered here are numerically integrated using the finite volume methodology. Because the solid surfaces for different shapes of the seat and reed do not coincide with the cylindrical coordinates employed in the domain discretization, use was made of the *Eulerian Lagrangian Algorithm For INterface Tracking* (ELAFINT). The ELAFINT methodology (Udaykumar *et al.*, 1996; Ye *et al.*, 1999) shapes the volumes with irregular format that are in the interface between fluid and solid. With this methodology the control volumes are regular and proper for discretization in cylindrical coordinates within the flow passages, and at the flow boundaries the volumes become trapezoidal to accommodate for the solid walls.

The present work is organized according to the present form: next section explores the partial differential equations that model the flow field across the valve and presents the four geometries used for the radial diffusers; section three validates the numerical solution and the ELAFINT methodology comparing dimensionless pressure profile obtained both numerically and experimentally; section four presents numerically determined effective flow and force areas; and in the last section some conclusions are offered.

2. Problem Formulation

The geometries of radial diffusers with modified parameters investigated in the present work are presented in Fig. 2. As the flow is axially symmetric, only one angle is studied along the diffuser circumference, simulating a bi-dimensional problem. The basic assumptions employed in simplifying the problem are isothermal, isocoric, steady laminar flow of newtonian fluid. Continuity and Navier-Stokes equations in axial and radial directions are the governing equations that describe the flow and can be written as,

$$\frac{\partial(\rho u)}{\partial x} + \frac{1}{r} \frac{\partial(\rho r v)}{\partial r} = 0 \quad (1)$$

$$\frac{\partial(\rho u u)}{\partial x} + \frac{1}{r} \frac{\partial(\rho r v u)}{\partial r} = \frac{\partial}{\partial x} \left(\mu \frac{\partial u}{\partial x} \right) + \frac{1}{r} \frac{\partial}{\partial r} \left(\mu r \frac{\partial u}{\partial r} \right) - \left(\frac{\partial p}{\partial x} \right) \quad (2)$$

$$\frac{\partial(\rho uv)}{\partial x} + \frac{1}{r} \frac{\partial(\rho r v v)}{\partial r} = \frac{\partial}{\partial x} \left(\mu \frac{\partial v}{\partial x} \right) + \frac{1}{r} \frac{\partial}{\partial r} \left(\mu r \frac{\partial v}{\partial r} \right) - \left(\frac{\partial p}{\partial r} \right) - \left(\frac{\mu v}{r^2} \right) \quad (3)$$

where ρ ($=1.205 \text{ kg/m}^3$) is the fluid density, μ ($=1.81 \times 10^{-5} \text{ Pa.s}$) is the absolute viscosity, u and v are, respectively, the axial and radial velocity components and p is the pressure. Equations (1) to (3) can be expressed by a single equation for the generic ϕ variable as,

$$\frac{\partial(\rho u \phi)}{\partial x} + \frac{1}{r} \frac{\partial(\rho r v \phi)}{\partial r} = \frac{\partial}{\partial x} \left(\Gamma^\phi \frac{\partial \phi}{\partial x} \right) + \frac{1}{r} \frac{\partial}{\partial r} \left(\Gamma^\phi r \frac{\partial \phi}{\partial r} \right) + S^\phi \quad (4)$$

where ϕ takes on the unitary value for Eq. (1), and u and v for Eqs. (2) and (3), respectively; Γ^ϕ and S^ϕ are the diffusion coefficients and source terms, respectively.

Attention will now be devoted to the boundary conditions that should be applied to the governing equations. At the outflow boundary local parabolic flow condition is applied, that is, $\partial(rv)/\partial r = u = 0$. At $r = 0$ the condition is $v = \partial u/\partial r = 0$. At the solid walls the non-slip condition is imposed, $v = u = 0$. At the entrance of the feeding orifice the axial velocity is determined from the prescribed Reynolds number, $u = U = \mu \text{Re}/(\rho d)$, and a null radial component of the velocity is imposed.

For the integration of the general governing differential equation, Eq. (4), using the finite volume methodology, the solution domain is divided in small non-overlapping control volumes. Next the differential equations are integrated along each control volume yielding a set of algebraic equations. The continuity equation is then transformed in an equation for pressure using the SIMPLE algorithm (Patankar, 1980), and the algebraic equations are solved by a Gauss-Seidel iterative procedure. It should be noted that when Eq. 4 is integrated along the control volumes that intercept the solid walls, the ELAFINT methodology (Udaykumar *et al.*, 1996; Ye *et al.*, 1999) is employed to capture the actual shape of the solid-fluid interface. Further details of the numerical methodology including a full description of ELAFINT can be found in Mariani (2002).

3. Validation of the Numerical Results

Validation of the numerical solution including the ELAFINT methodology is performed comparing computational and experimental pressure profiles along the valve reed for a situation where the valve is inclined 5° with respect to the horizontal position, as depicted in Fig. 3. The valve parameters for the situation in the figure are $rp_1 = 58$; $d = 34.9$; $e = 14.5$ and $D = 104.7$, where all dimensions are in millimeters.

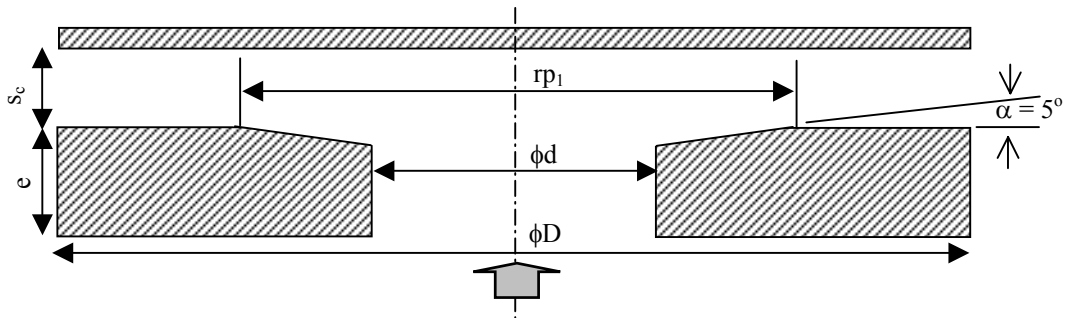


Figure 3. Valve seat with inclination of 5° .

Figures 4 and 5 present numerical and experimental results for the dimensionless pressure profiles along the valve reed. The dimensionless pressure is defined as $2p/(\rho U^2)$ and is presented as a function of two dimensionless distance between valve seat and valve reed ($s_c/d = 0.012$ and 0.020), and two Reynolds numbers ($\text{Re} = 1000$ and 2500). The experimental results were obtained from an existing experimental setup which was employed in previous investigations (see for instance Ferreira *et al.*, 1989).

Overall a good agreement prevailed between computation and experiment, except at the stagnation region. The agreement for $s_c/d = 0.020$ tend to be better than that for $s_c/d = 0.012$. It should be pointed out that because of the small distance between the valve seat and reed, very high gradients are encountered for both pressure and velocity fields. Those gradients impose many difficulties in solving the differential equation as well as in performing accurate experiments. For a description of the experimental uncertainty and the pressure sensitivity to small changes in the diffuser geometry the interested reader is referred to Ferreira *et al.* (1989). According to Ferreira *et al.*, 1989 it is most likely that the large deviation between experiment and computation observed in the flat region of Figs. 4 and 5 are due

to experimental difficulties, specially considering that a mesh refinement did not improved the numerical results at this region.

Worth noting is the good agreement observed between experiment and computation in the flow acceleration region, especially at higher gaps between valve seat and reed. A last aspect to be noted in Figs. 4 and 5 is the pressure oscillation verified in the experimental results. Those oscillations may suggest some kind of flow instability which has not been observed before (Prata *et al.*, 1995, Ferreira *et al.*, 1989, Possamai *et al.*, 2001, Deschamps *et al.*, 2000). Those oscillations increased with increasing values of the gap between valve seat and reed.

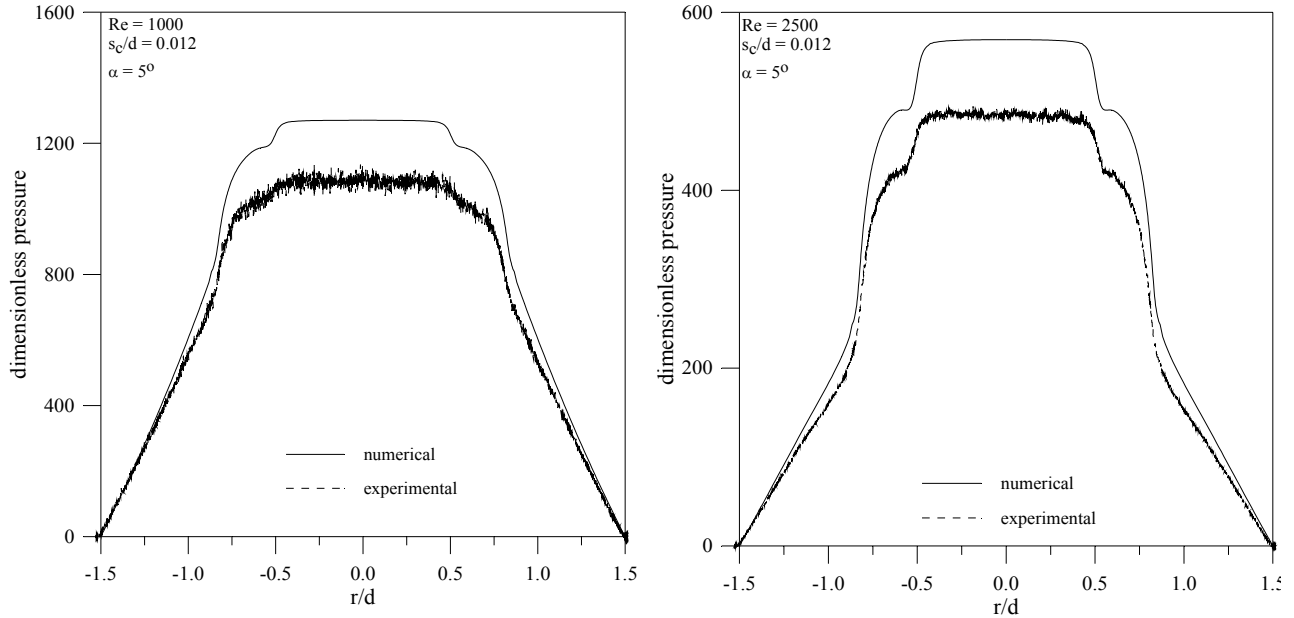


Figure 4. Numerical and experimental results for pressure distribution along valve reed for $Re = 1000$ and 2500 , $s_c/d = 0.012$ and $\alpha = 5^\circ$.

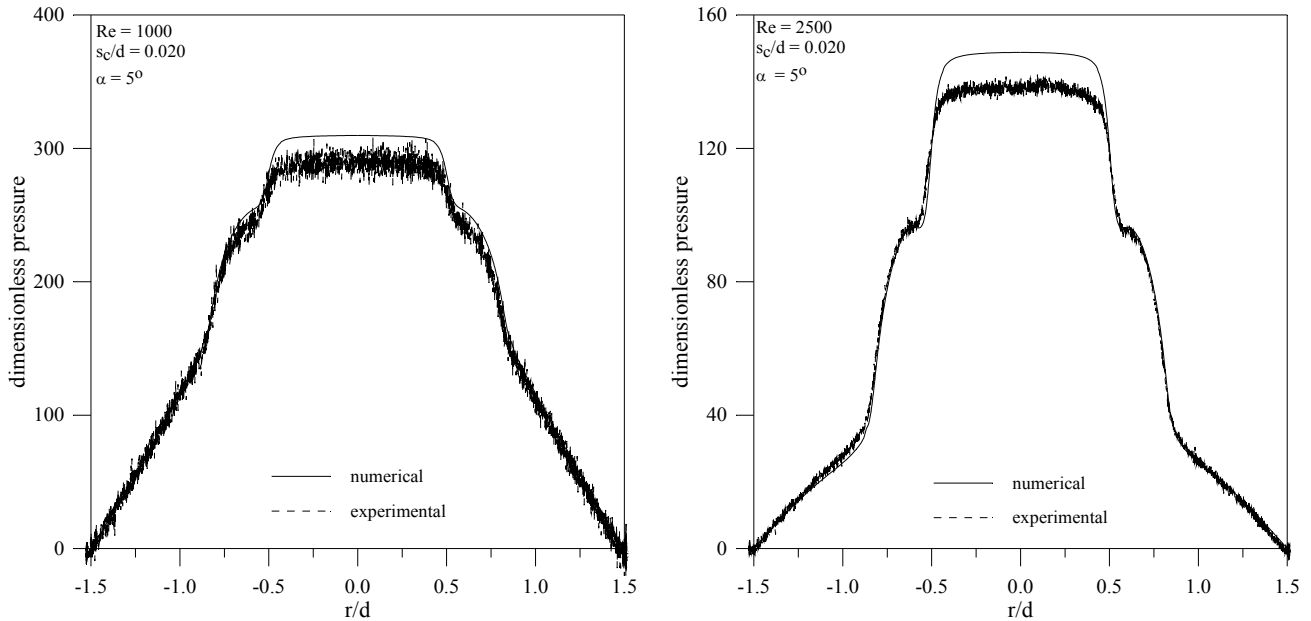


Figure 5. Numerical and experimental results for pressure distribution along valve reed for $Re = 1000$ and 1500 , $s_c/d = 0.020$ and $\alpha = 5^\circ$.

4. Effective Flow and Force Areas

As explored before, two parameters are very important in valve modeling and design: the effective flow and force areas. Those two parameters are generally used in numerical simulation of reciprocating hermetic compressors and can also be employed to evaluate the efficiency of the valves.

The effective flow area, A_{ee} , is directly related to the pressure drop through valve. For a given pressure drop A_{ee} can yield the mass flux through the valve. Thus, the higher the A_{ee} , the better is the performance of the valve with respect to the flow through it (Ussyk, 1984). The effective flow area is defined as

$$A_{ee} = \frac{\dot{m}}{p_u \sqrt{\frac{2k}{(k-1)RT_u}} \sqrt{r_p^{2/k} - r_p^{(k+1)/k}}} \quad (5)$$

where \dot{m} is the mass flow rate through the valve, $r_p = p_{atm}/p_u$, p_{atm} is the atmospheric pressure, p_u is the pressure upstream the valve, $k = c_p/c_v$, R is the gas constant, and T_u is the temperature upstream the valve.

Results for the dimensionless effective flow area ($A_{eea} = 4A_{ee}/\pi d^2$) are shown in Tab. 1 for the different diffuser geometries explored and for $s_c/d = 0.012$ and 0.020 . To serve as a basis for comparisons the first line of results are for the standard geometry of the valve, with no angle or rounding. As observed from the table, increase in the Reynolds number results in increase of the dimensionless effective flow area. Furthermore, for each Re and s_c/d values, the valve modification either due to the angle or to the rounding increased the dimensionless effective flow area. For the dimensionless distance 0.012 , the most expressive increasing of the effective flow area was obtained for the simultaneous 5° inclination of the seat and reed. The use of the radius rounding enhances the effective flow area, but to a less extend the use of the inclination.

Table 1. Dimensionless effective flow and force area.

Variation of geometric parameters	Re	$s_c/d = 0.012$		$s_c/d = 0.020$	
		A_{eea}	A_{efa}	A_{eea}	A_{efa}
no inclination or no radius rounding	1000	0.02133	2.868	0.04418	2.459
	1500	0.02533	2.558	0.05160	2.012
	2000	0.02839	2.276	0.05693	1.624
	2500	0.03086	2.021	0.06093	1.286
5° seat inclination	1000	0.02807	4.312	0.05693	3.730
	1500	0.03374	4.062	0.06761	3.339
	2000	0.03823	3.828	0.07571	2.995
	2500	0.04196	3.612	0.08231	2.691
5 [mm] seat radius rounding	1000	0.02510	3.654	0.05066	3.167
	1500	0.03026	3.403	0.06023	2.785
	2000	0.03442	3.170	0.06767	2.451
	2500	0.03793	2.955	0.07374	2.158
5° seat and reed inclination	1000	0.02867	4.252	0.05619	3.660
	1500	0.03432	4.003	0.06625	3.273
	2000	0.03898	3.798	0.07385	2.945
	2500	0.04391	3.673	0.07992	2.669
5 [mm] seat and reed radius rounding	1000	0.02443	3.571	0.05034	3.142
	1500	0.02923	3.297	0.05955	2.747
	2000	0.03304	3.052	0.06659	2.406
	2500	0.03626	2.833	0.07224	2.111

The effective flow area is important in predicting the mass flow rate through the valve during suction and discharge. However, to calculate the valve movement it is necessary to know the force acting on the reed during each instant of time. This force is a result of the difference in pressure acting on both sides of the valve and depends on the flow and on the opening of the reed (Schwartzler and Hamilton, 1972). Usually the force on the valve is calculated through the effective force area, defined as,

$$A_{ef} = F/\Delta p_v \quad (6)$$

where Δp_v is the pressure difference through the valve.

Results for the dimensionless effective force area ($A_{efa} = 4A_{ef}/\pi/d^2$) are presented in Tab. 1. As in the case of A_{eea} , the effective force area increases with the Reynolds number and with the gap between valve seat and reed. With respect to the standard geometry with no angle and rounding, it is noticed that for $s_c/d = 0.020$, turning the seat 5° the dimensionless effective force area is enhanced by approximately 52%, 66%, 84% and 109% for the Reynolds numbers equal to 1000, 1500, 2000 and 2500, respectively. The largest values of A_{efa} were obtained with the 5° inclination of the seat; the others geometry modifications also increased A_{efa} , but the increase was not so expressive. As observed from the table, the dimensionless effective force area is more effectively influenced by the Reynolds number and by the modifications in the geometric parameters than the dimensionless effective flow area.

Figures 6 to 9 present numerical values of the dimensionless effective flow area for $s_c/d = 0.012$ and 0.020 as a function of the four geometric modifications on the radial diffuser, that is, seat inclination, seat rounding, seat and reed inclination, and seat and reed rounding, having the Reynolds number as curve parameter. In general, the dimensionless effective flow area increases with the increasing value of the geometric modifications and of the Reynolds numbers. The presence of the seat inclination at the outlet of the feeding orifice provides a substantial increase in the dimensionless effective flow area, as observed in Fig. 6. This result was also observed by Puff *et al.* (1992), and can be explained noticing that the presence of the chamfer decelerates the fluid at the outlet of the feeding orifice which in turn increases the pressures by the Bernoulli effect.

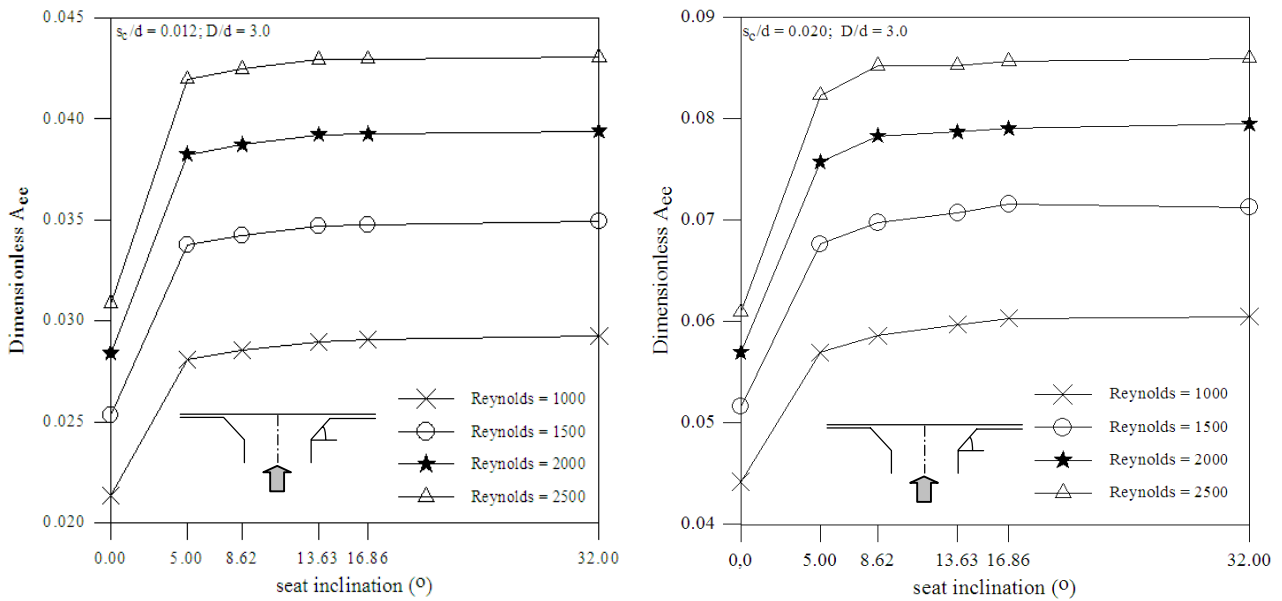


Figure 6. Influence of inclination seat on the dimensionless effective flow area.

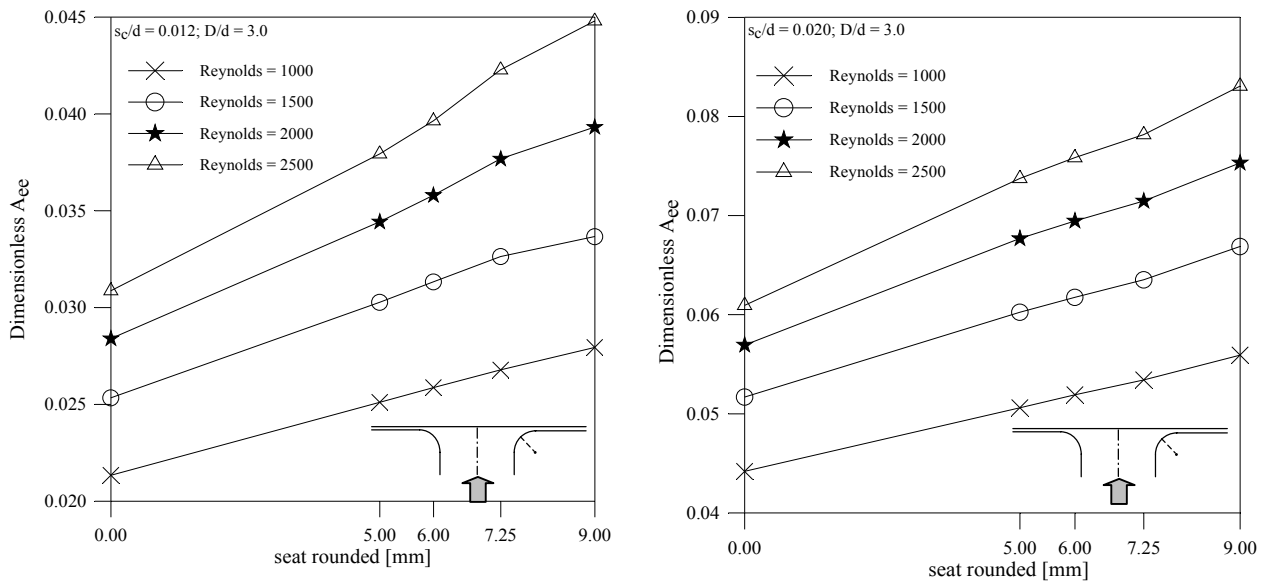


Figure 7. Influence of seat rounded on the dimensionless effective flow area.

In Figs. 6 and 8 it is observed that the use of the inclination results in expressive augmentations of the effective flow area when the angle changes from 0° to 5° . However, for inclinations larger than 5° little influence is observed in the A_{eff} value, especially for $s_c/d = 0.012$, no matter which Reynolds number is considered. Figures 7 and 9 show the dimensionless effective flow area for varying radius values of the seat round edge. For all situations investigated the dimensionless effective flow area exhibits a monotonic increase as the seat radius increases, that is so for the two spacing and all Reynolds numbers explored.

From the results it is observed that, in general, the dimensionless effective flow area is largely influenced by the Reynolds numbers, the spacing between valve seat and reed and shape modifications.

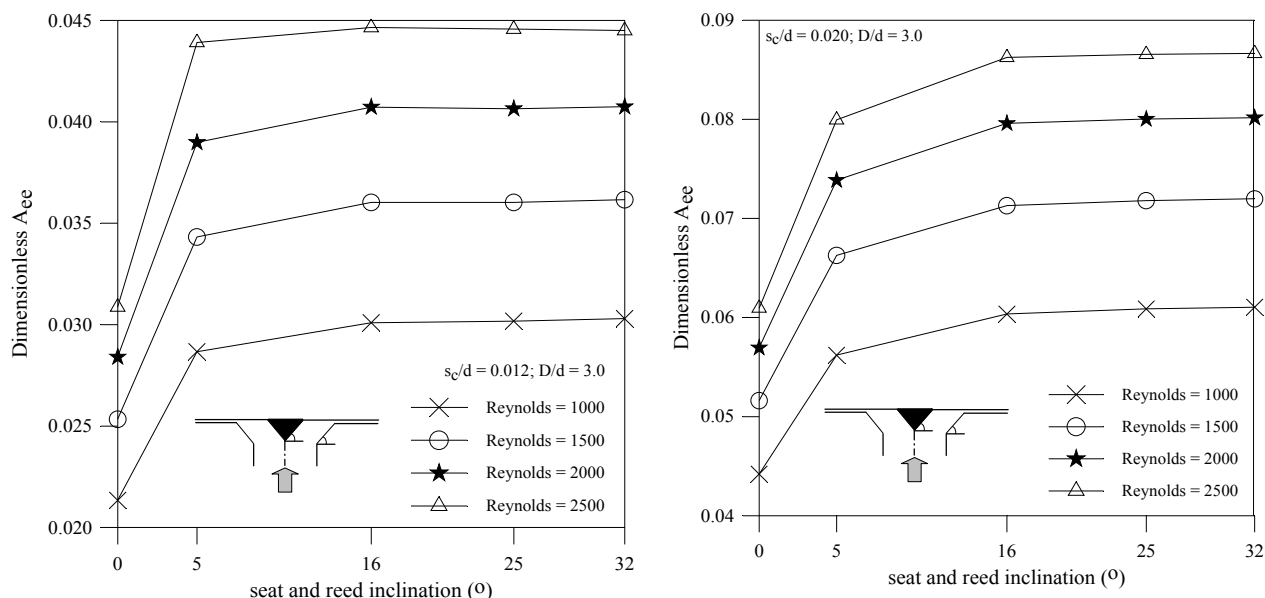


Figure 8. Influence of seat and reed inclination on the dimensionless effective flow area.

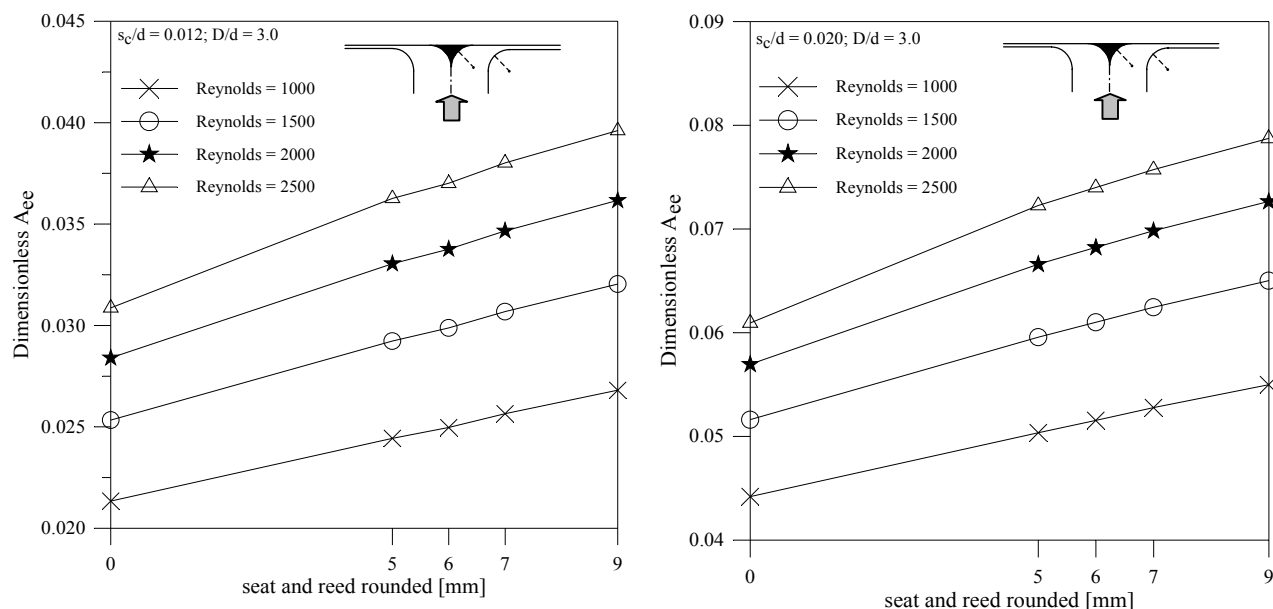


Figure 9. Influence of seat and reed rounded on the dimensionless effective flow area.

Figures 10 to 13 show the variation of the dimensionless effective force area for $s_c/d = 0.012$ and 0.020 as a function of the geometry modifications, for Reynolds numbers varying from 1000 to 2500. For both spacing between seat and reed, $s_c/d = 0.012$ and 0.020 , the dimensionless effective force area exhibits a monotonic behavior similar to that observed for the effective flow area, that is, as the modification parameter increases the effective force area increases. As seen in the figures, the use of inclination at the orifice outlet causes an increase in the effective force area which has a reduced impact for larger values of the inclination angle. Regarding the radius of the seat round edge, as the radius value increases the dimensionless effective force area increases without showing any tendency to become less influenced by modifications on the radius.

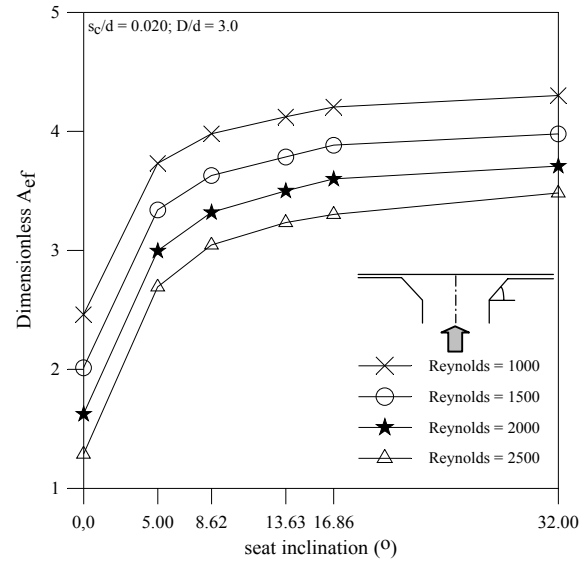
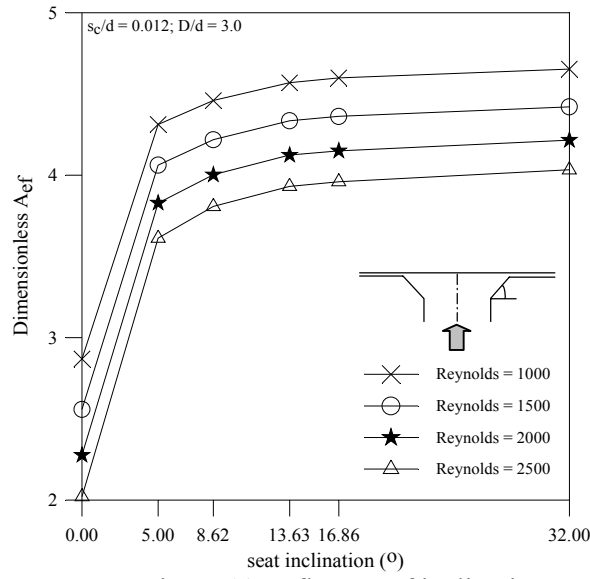


Figure 10. Influence of inclination seat on the dimensionless effective force area.

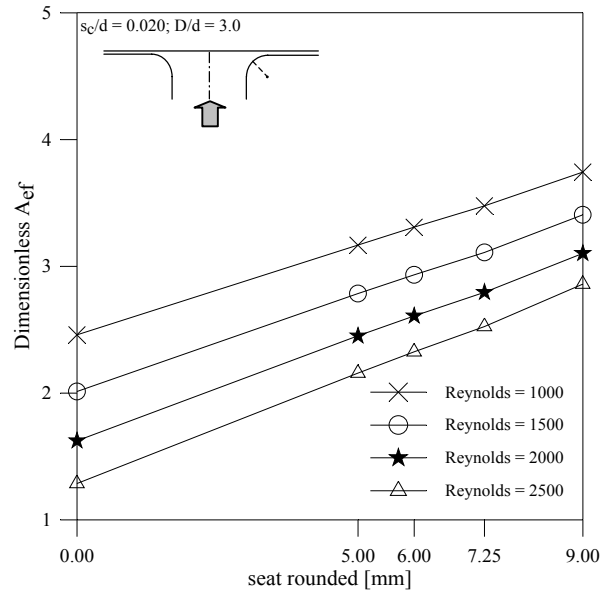
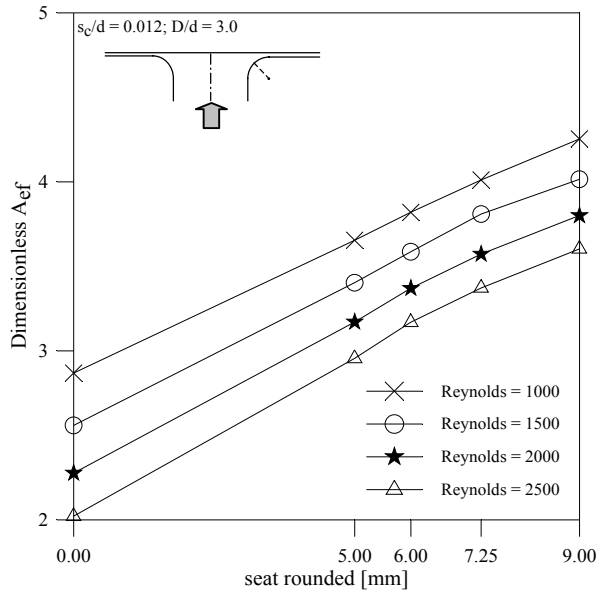


Figure 11. I Influence of seat rounded on the dimensionless effective force area.

As shown in Figs. 10 to 13, the effective force area decreases as the Reynolds number increases. At a first sight this result may appear strange since the effective force area is directly proportional to the force on the valve reed and that increase with an increase in the Reynolds number. However, in conformity with Eq. 6, it is seen that as the Reynolds number increases the increase of the pressure difference across the valve is more expressive than the increase of the resultant force on the reed, yielding a reduction in the effective force area.

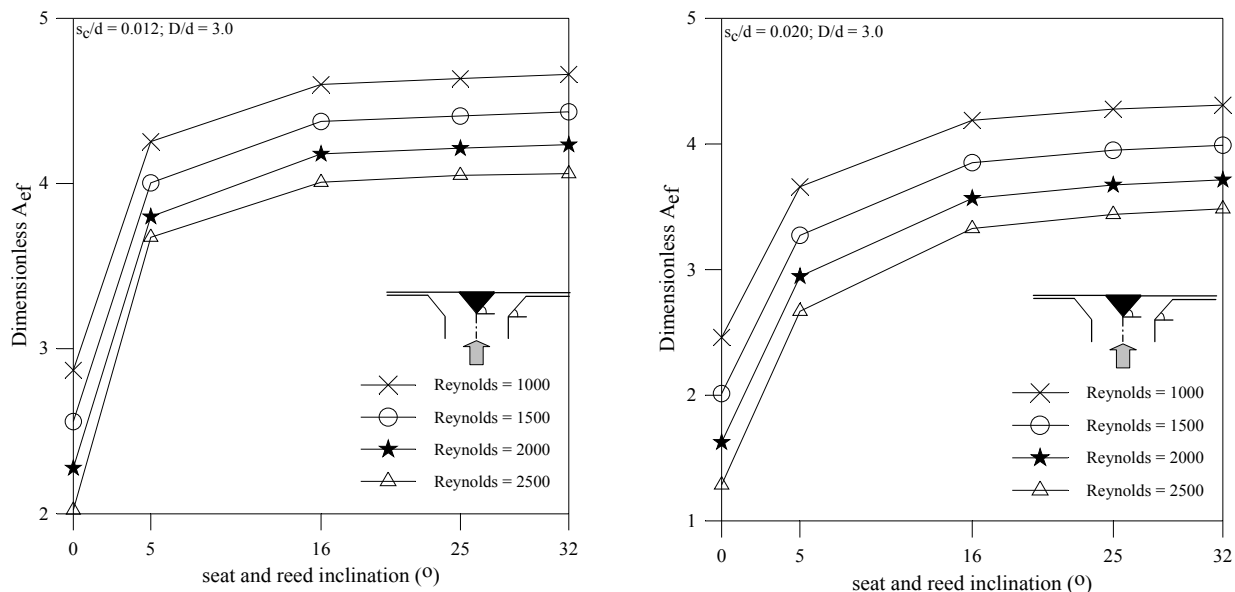


Figure 12. Influence of seat and reed inclination on the dimensionless effective force area.

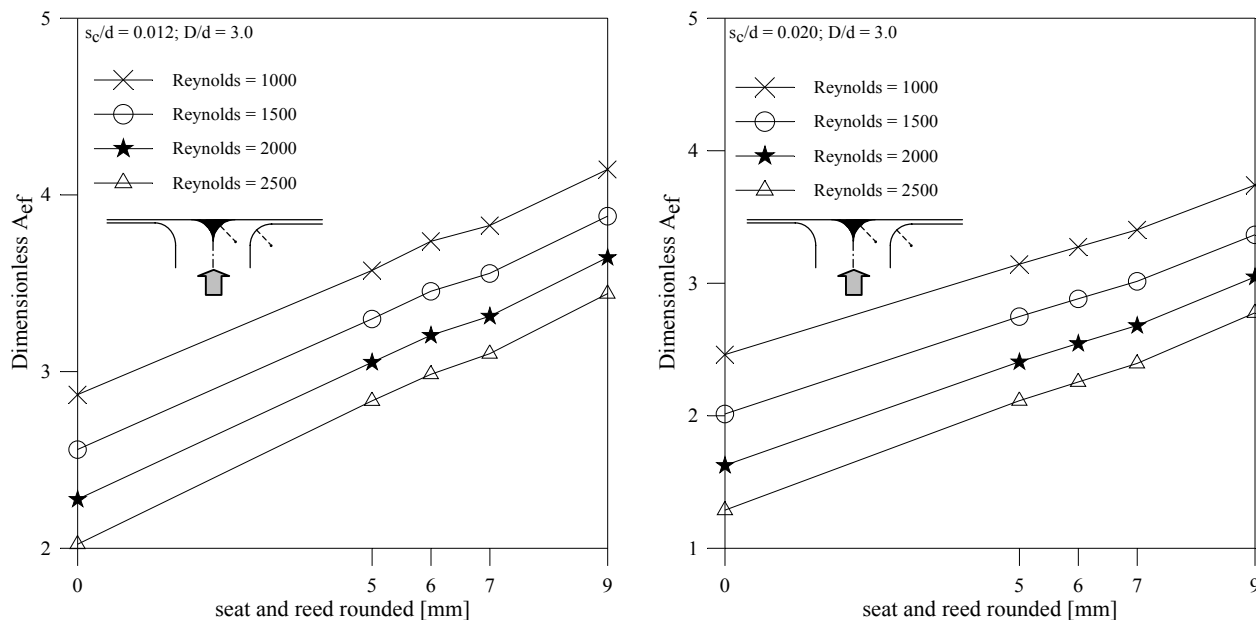


Figure 13. Influence of seat and reed rounded on the dimensionless effective force area.

5. Conclusions

The current work numerically investigated the steady laminar isocoric isothermal axis-symmetrical flow in radial diffusers. This geometry approximates the geometry of automatic valves in reciprocating hermetic compressors which is the most common compressor employed in domestic refrigerators. Performance of those valves is entirely controlled by the flow itself, and for designing purposes it is convenient to express the mass flow rate through the valves and the force acting on their reed in terms of two parameters known as effective flow and force areas. The present work explored the impact that small geometric changes on the valve have on the effective flow and force areas. The changes made on the valve geometry were seat inclination, seat rounding, seat and reed inclination, and seat and reed rounding.

For the flow solution, use was made of the finite volume methodology. Cylindrical coordinates were employed for writing the governing differential equation, and to handle the irregular geometry of the diffuser the ELAFINT procedure was implemented. Validation of the numerical solution was performed comparing the pressure distribution on the valve reed obtained experimentally with the corresponding pressure values obtained computationally and reasonable to good agreements were observed.

The current analysis concluded that small modifications on the valve geometry such as seat inclination, seat rounding, seat and reed inclination, and seat and reed rounding, cause a significant increase in effective flow and force

areas. For example, a seat inclination of only 5° is capable of altering the effective flow area by 30 % which is an expressive change.

Simultaneous use of inclination or rounding radius at the valve seat and valve reed tend to cause lesser changes in the effective flow and force areas if compared to inclination or radius rounding separately at the seat. Seat modifications, in general, are more easily implemented than reed modifications and are very beneficial to the valve performance.

6. Acknowledgments

This work is part of a technical-scientific cooperation program between Federal University of Santa Catarina and the Brazilian Compressor Industry, EMBRACO. The support of CAPES in providing a scholarship for the first author is greatly appreciated.

7. References

- Deschamps, C. J., Prata, A. T., Ferreira, R. T. S., 2000, "Modeling of turbulent flow through radial diffuser", *Journal of the Brazilian Society of Mechanical Sciences*, Vol. XXII, no. 1, pp. 31-41.
- Ervin, J. S., Suryanarayana, N. V., Ng, H. C., 1989, "Radial, turbulent flow of a fluid between two coaxial disks", *ASME Journal Fluids Eng.*, Vol. 111, pp. 378-383.
- Ferreira, R. T. S., Driessen, J. L., 1986, "Analysis of the influence of valve geometric parameters on the effective flow and force areas". In: Ninth Purdue Compressors Technology Conference West Lafayette, USA, pp. 632-646.
- Ferreira, R. T. S., Deschamps, C. J., Prata, A. T., 1989, "Pressure distribution along valve reeds of hermetic compressors", *Experimental Thermal and Fluid Sciences*, Vol. 2, pp. 201-207.
- Hayashi, S., Matsui, T. and Ito, T., 1975, "Study of flow and thrust in nozzle-flapper valves", *ASME Journal Fluids Eng.*, Vol. 97, pp. 39-50.
- Mariani, V. C., 2002, "Methods of optimization and interface modeling techniques for analysis of fluid flow in radial diffuser with irregular geometries", Thesis (in portuguese), Department of Mechanical Engineering, Federal University of Santa Catarina, Brazil.
- Patankar, S. V., 1980, "Numerical Heat Transfer and Fluid Flow", McGraw-Hill.
- Possamai, F. C., Ferreira, R. T. S., Prata, A. T., 2001, "Pressure distribution in laminar radial flow through inclined disks", *International Journal of Heat and Fluid Flow*, 22, pp. 440-449.
- Prata, A. T., Ferreira, R. T. S., 1990, "Heat transfer and fluid flow considerations in automatic valves of reciprocating compressors", *Proceedings of the 1990 International Compressor Engineering Conference*, West Lafayette, USA, Vol. 1, pp. 512-521.
- Prata, A. T., Pilichi, C. D. M., Ferreira, R. T. S., 1995, "Local heat transfer in axially feeding radial flow between parallel disks", *ASME Journal Heat Transfer*, Vol. 117, pp. 47-53.
- Puff, R., Prata, A. T. and Ferreira, T. S., 1992, "Effective flow and force areas for different geometries of compressor valves with laminar flow", 4th Brazilian Congress of Thermal Engineering and Sciences, ENCIT, Rio de Janeiro, pp. 537-540.
- Schwerzler, D. D., Hamilton, J. F., 1972, "An Analytical for Determining Effective Flow and Force Areas for Refrigeration Compressor Valving Systems", *International Compressor Engineering Conference at Purdue*, West Lafayette, Indiana, Vol. I, pp. 30-36.
- Tabatabai, M., Pollard, A., 1987, "Turbulence in radial flow between parallel disks at medium and low Reynolds numbers", *Journal Fluid Mechanics*, Vol. 185, pp. 483-502.
- Udaykumar, H. S., Shyy, W., Rao, M. M., 1996, "ELAFINT: A Mixed Eulerian-Lagrangian Method for Fluid Flows with Complex and Moving Boundaries", *International Journal for Numerical Methods in Fluids*, Vol. 22, pp. 691-712.
- Ussyk, M. S., 1984, "Simulação Numérica do Desempenho de Compressores Herméticos Alternativos", *Dissertação de Mestrado. Departamento de Engenharia Mecânica, UFSC*.
- Ye, T., Mittal R., Udaykumar, H. S., Shyy, W., 1999, "An accurate cartesian grid method for viscous incompressible flows with complex immersed boundaries", *Journal of Computational Physics*, Vol. 156, pp.209-240.